ERTMS/ETCS Virtual Coupling: Proof of Concept and Numerical Analysis

Carlo Di Meo, Marco Di Vaio, Francesco Flammini, *Senior Member, IEEE*, Roberto Nardone, Stefania Santini, *Member, IEEE*, and Valeria Vittorini

***Abstract*— Railway infrastructure operators need to push their network capacity up to their limits in high-traffic corridors. Virtual coupling is considered among the most relevant innovations to be studied within the European Horizon 2020 Shift2Rail Joint Undertaking as it can drastically reduce headways and thus increase the line capacity by allowing to dynamically connect two or more trains in a single convoy. This paper provides a proof of concept of Virtual coupling by introducing a specific operating mode within the European rail traffic management system/European train control system (ERTMS/ETCS) standard specification, and by defining a coupling control algorithm accounting for time-varying delays affecting the communication links. To that aim, we define one ploy to enrich the ERTMS/ETCS with Virtual coupling without changing its working principles and we borrow a numerical analysis methodology used to study platooning in the automotive field. The numerical analysis is also provided to support the proof of concept with quantitative results in a case-study simulation scenario.**

***Index Terms*— Railways, ERTMS/ETCS, automatic train control, virtual coupling, simulation, numerical analysis.**

I. Introduction

THE European Railway Traffic Management System/ European Train Control System (ERTMS/ETCS, or simply ERTMS hereinafter) [1] is an international standard aimed at improving interoperability and performance of modern railways. After several years of experience with ERTMS development, the railway industry is tackling the challenge of improving the standard and designing the new generation railway control systems. In order to foster coordination of research and innovation efforts, the European Shift2Rail Joint Undertaking has been established under Horizon 2020 [2]. Shift2Rail has devoted an entire pillar of its programme (i.e. IP2, advanced Traffic Management and Control System) to enhance capacity and reliability through improved management of signalling and supervision systems. One important step in this direction is to increase rail capacity by introducing moving block signalling. Some pilot ERTMS installations exist implementing moving block signalling although such experiences are very limited to date [3]. The Shift2Rail IP2 addresses research in the field of moving block signalling and also goes a step further by introducing the concept of *Virtual Coupling*.

Virtual Coupling could be a ground-breaking innovation in railways as it enables coupling/uncoupling of train *convoys* by drastically reducing headways. That opens a completely new scenario in which cooperative driving could be exploited based on Train-to-Train communication and distributed control, in order to achieve a global coordination of virtually-coupled convoys via wireless communication. The contribution of this paper is twofold: firstly, it provides technical hints to introduce and evaluate Virtual Coupling in the context of ERTMS; secondly, it provides a numerical analysis of rail vehicle cooperation and platooning strategies borrowed from the automotive domain in order to perform a preliminary evaluation of feasibility and performance. In this study, we assume to enrich ERTMS with Virtual Coupling instead of defining a fully new signalling system, which is the preferred approach to ensure backward compatibility and minimize the impact on existing infrastructures since it guarantees the re-use of standard operating modes and related safety mechanisms. Based on that assumption, we define and evaluate a coupling control strategy that is robust against communication impairments. The closed-loop exponential stability is analytically proved for this control strategy by exploiting a proper Lyapunov-Krasovskii functional that extends to a network of dynamical systems in presence of multiple delays the approach proposed in [4] for a single time-delayed system. A realistic case study is introduced to perform simulations and provide some insights about the possibility of actuating platoons of trains. Although the evaluation results reported in this paper are dependent on the specific simulation scenario, the methodology we introduce is generic and applicable to diverse train speeds and configurations.

This paper is organized as follows. Section II contains a brief overview of ERTMS concepts and terminology as well a discussion about related works. Section III discusses how to extend ERTMS with Virtual Coupling and some reliability-related implications. Section IV introduces the coupling control strategy for cooperative driving and platooning in ERTMS. Section V reports simulation results in the example scenario.

Manuscript received May 31, 2018; revised December 21, 2018 and April 16, 2019; accepted May 17, 2019. Date of publication June 17, 2019; date of current version May 29, 2020. This work was partially supported by the Department of Electrical Engineering and Information Technologies (DIETI) of the University of Naples Federico II within the project MOdel-Driven AnaLysis of Critical Industrial Systems (MODAL). The Associate Editor for this paper was X. Cheng. *(Corresponding author: Roberto Nardone.)*

C. Di Meo, M. Di Vaio, R. Nardone, S. Santini, and V. Vittorini are with the Department of Electrical Engineering and Information Technology (DIETI), University of Naples Federico II, 80125 Naples, Italy (e-mail: carlo.dimeo@unina.it; marco.divaio@unina.it; roberto.nardone@unina.it; stsantin@unina.it; valeria.vittorini@unina.it).

F. Flammini is with the Department of Computer Science and Media Tech-nology, Linnaeus University, 351 95 Växjö, Sweden (e-mail: francesco.flammini@lnu.se).

Digital Object Identifier 10.1109/TITS.2019.2920290

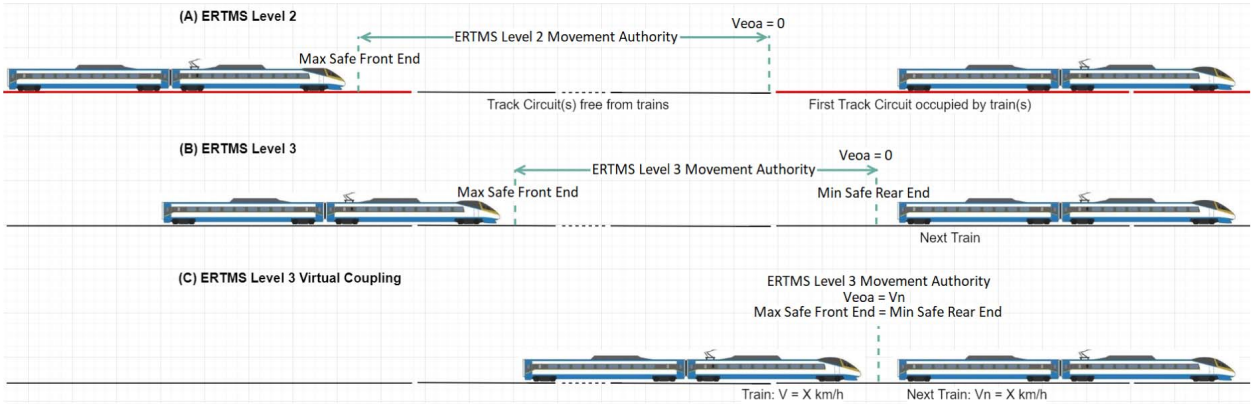

Fig. 1. (a) ERTMS Level 2 - Fixed Block; (b) ERTMS Level 3 - Moving Block; (c) ERTMS Level 3 + Virtual Coupling.

Finally, Section VI provides some closing remarks and hints about future developments.

II. Background and Related Work

A. ERTMS Levels

The ERTMS standard defines the functional architecture, technologies and message format to ensure safe communication between train onboard and trackside equipment. The specifications identify three levels of growing complexity that can be implemented singularly or jointly.

- ERTMS Level 1. At this level, communication is discontinuous and based on signals transmitted by the so-called Euro-balises that are devices installed between track lines. Some additional mechanisms (i.e., infill) can be used to make signalling semi-continuous, but ERTMS Level 1 cannot guarantee the capacity of higher levels due to technology limitations, and it is therefore out of the scope of this work.
- ERTMS Level 2. This level implements *continuous radio signalling* based on the EURORADIO safe protocol via the Global System for Mobile Communications - Railway (GSM-R). The exact positions of the trains and all the other necessary information are automatically transmitted at periodical intervals and/or upon events. The movement authority is transmitted to the train at any time together with all the information related to speed profiles associated to track characteristics, conditions, speed restrictions, etc.
- ERTMS Level 3 implements moving block instead of fixed block signalling. This allows for the definition of movement authorities regardless of fixed block sections according to the traffic conditions. As a consequence, this level is able to maximize track capacity.

The trackside controller responsible for train separation is named Radio Block Center (RBC). The distance each train can cover in safe conditions is named Movement Authority (MAs) and it is computed by the RBC based on train position and track conditions. The end of the MA is named *end of authority* (eoa) and the allowed speed at the end of authority is named Veoa. MAs allow the on-board European Vital Computer (EVC) to compute the *dynamic speed profile* and braking curves. The speed profile is used to set train maximum speed depending on forward track conditions (speed restrictions, distance from the preceding train, etc.).

At ERTMS Level 3, the MA is computed by considering the actual distance between trains, while at Level 2 the occupation status of the so-called *track circuits* must be detected (see Fig. 1a and Fig. 1b). Hence, Level 3 allows the removing of the track segmentation into fixed blocks. It is rather intuitive that Level 3 provides higher capacity compared to Level 2 due to shorter headways, at the expense of additional train integrity check mechanisms. The new paradigm of *Virtual Coupling* we address in this paper has been associated by some analysts to a future *ERTMS Level 4* [5], although there is currently no reference to that level in the official ERTMS documents. Virtual Coupling allows trains to join and increase line capacity due to extremely short headways (Fig. 1c). In this paper, we suggest a simple way of implementing Virtual Coupling in the context of ERTMS by assigning the following train a release speed at *Veoa* that is equal to the speed of the preceding train. Such a mechanism can be managed by the RBC based on the position reports received from the trains and including current train speeds. Together with the need for the specification of a further ERTMS level and/or on-board operating mode, the real implementation of Virtual Coupling poses additional challenges in terms of reliability and safety that need to be investigated extensively before such a system can become operational.

B. Related Works

Virtual Coupling is a recent concept that is still far from being implemented and as such it represents an open research challenge in the railway domain. The transition towards ERTMS Level 3 moving block signalling has been very slow due to its benefits probably not justifying transition costs and additional risks to be managed. A number of solutions are currently being developed at different levels and the expected benefit of adding Virtual Coupling on top of ERTMS Level 3 is considered crucial for the future implementation of the standard [3]. A few recent reports from international railway organizations and professional institutions introduce the idea of Virtual Coupling in general terms [2], [5]. The Shift2Rail Joint

Undertaking Multi-Annual Action Plan [2] also states that "virtual trains" represent "a total deviation from the traditional railway operational concept" and proposes that any investigation "starts from the current interoperable signalling system" (i.e., ERTMS). The report published by IRSE (Institution of Railway Signal Engineers) [5] discusses the Virtual Coupling concept and poses some questions about its safety and benefits. A few recent works address the technologies required for the implementation of Virtual Coupling (for example see [6]). Virtual Coupling heavily depends on wireless communication, hence works addressing innovative technologies for railway communications also mention Virtual Coupling and Train-to-Train communication as promising applications (e.g., see [7]–[10]). To the best of our knowledge, no studies have been published yet which provide hints for implementation of Virtual Coupling on top of ERTMS Level 3 leveraging on existing ERTMS "language" (variables, packets, messages) and evaluate feasible *control strategies* in realistic scenarios, as we do in this paper. However, a new transportation paradigm is emerging for connected ground vehicles, such as cars, moving according to platoon-based driving patterns. To cope with all the challenges and uncertainties arising from vehicle cooperation, platooning has already been investigated from different control perspectives in road transportation scenarios (e.g., see [11]–[14] and reference therein for a survey of the topic including communication constraints and related hardware solutions). The analysis performed in this paper also investigates the portability of some results achieved in cooperative driving and car platooning to the railway domain. Safety and reliability issues are only partially addressed by this study, as additional research is needed to consider all the relevant factors [5].

III. Virtual Coupling in ERTMS

A. Extending the On-Board Operating Modes

We have mentioned that ERTMS Level 3 is suitable to achieve very high capacity on high traffic corridors; however, its upgrade to Virtual Coupling while keeping backward compatibility with existing infrastructures would ensure their full exploitation. In ERTMS, Operating Modes are defined for the on-board European Vital Computer (EVC) according to the status of the track in order to guarantee adequate safety levels [1]. The Full Supervision operating mode is enabled when all information data required for complete train supervision is available. Partial Supervision (PS) is used when some information is missing and includes the specific Shunting, On-Sight and Staff Responsible modes. For the purposes of this discussion, we will only distinguish between FS and PS. As already mentioned, in this study we assume to implement Virtual Coupling by adding a further ERTMS Level 3 Operating Mode on top of Full Supervision. The new Operating Mode would be named "Full Supervision plus Virtual Coupling" (FSVC). In order to switch from FS to FSVC, the ERTMS infrastructure should check and guarantee that all the necessary conditions are fulfilled, including sufficient MA assigned to the preceding train, sufficient MA overlap between preceding and following train to ensure same routing in stations, successful

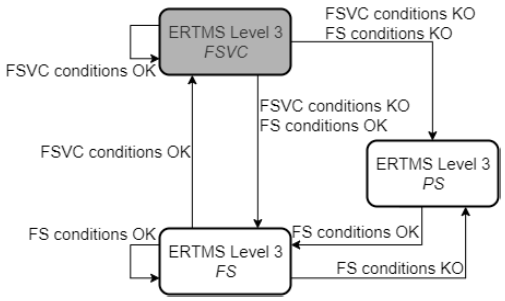

Fig. 2. Extended ERTMS Level 3 operating modes.

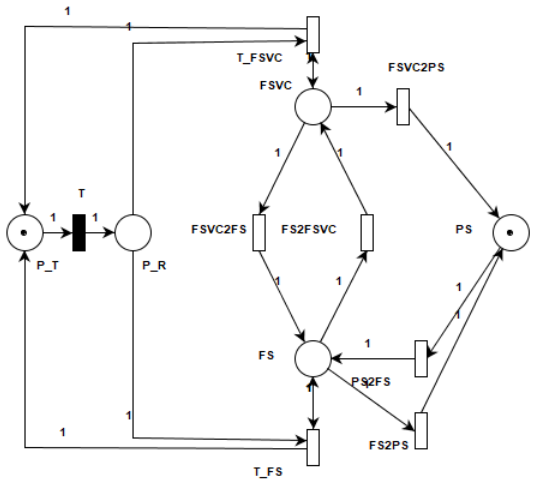

Fig. 3. Theoretical performability model.

establishment of Train-To-Train communication, etc. It is not in the scope of this paper to define all the additional FSVC safety requirements that should derive from the hazard analysis. If the infrastructure cannot guarantee all the required safety conditions, then ERTMS must fall back to FS, provided that its conditions are fulfilled, otherwise it must switch to PS (see Fig. 2). No direct switching from PS to FSVC should be possible. In FSVC, the EVC should always apply the most restrictive speed profile (MRSP) between the one provided by the RBC and the one provided by the preceding train through train-to-train communication. Hence, one of the advantages of the approach based on the additional FSVC operating mode is that the underlying safety and reliability conditions ensured by ERTMS remain unchanged. In FSVC, all the safety conditions related to trackside status, like speed restrictions, emergencies, route failures, etc., are still checked and supervised by the RBC. Regarding MA and MRSP computation derived by train-to-train communication, it is expected that a critical factor will be the capacity of the system to quickly and regularly update MA to trains so that they will not be obliged to slow down and disconnect from the preceding trains. Therefore, if the communication infrastructure ensures enough throughput and reliability such that the $T\_NVCONTACT$ timer used for vitality checking can be set to sufficiently low values (below 1s), then safety concerns will be automatically cleared.

B. Performability Issues

The transitions among the ERTMS operating modes discussed above can be modeled by the Petri Net in Fig. 3.

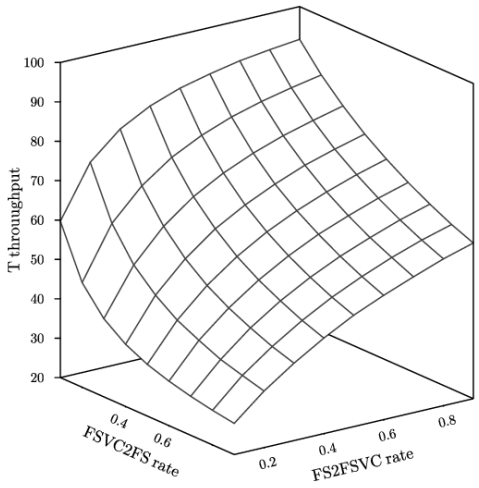

Fig. 4. Results of FSVC performability evaluation.

The delays associated to the stochastic transitions representing mode changes have a negative-exponential distribution. That assumption is realistic since those transitions represent time-to-fail (i.e., moving from higher to lower supervision) and time-to-repair (i.e., moving from lower to higher supervision) whose stochastic variables are demonstrated in the reliability theory to be well-modeled by negative exponential distributions. The transitions *T_FSVC* and *T_FS* have deterministic firing rates as they represent the frequency of trains stably running in FSVC and FS, respectively. The places *P_T* and *P_R* and the transition *T* have been added to evaluate the train frequency as a function of sojourn times in FSVC, FS and PS. Specifically, the throughput of transition *T* provides an upper bound to the number of trains the system is able to manage in the time unit (i.e., theoretical system capacity) as a function of model parameters. As an example, if we assume the trains running at 300 km/h on the Milano-Bologna high-speed ERTMS track in Italy, with realistic MAs at full speed of 15 km, then the maximum frequency would be $15/300 = 0.05$ h (i.e., 3 minutes minimum dispatching time).

At FSVC, the distance between trains will be given by the train minimum/maximum safe rear/front ends that are the train extremes augmented by the odometric errors. We assume an inter-distance of 3 km at 300 km/h, which correspond to a frequency of $3/300 = 0.01$ h (i.e., 36 seconds minimum dispatching time).

Performability model evaluation results are shown in Fig. 4. Without FSVC, the *T* frequency would be 20 trains per hour that is one train each 3 minutes. Such theoretical minimum is the closest corner in the graph (i.e., lowest point), where the rate of the transition towards FS is higher and the rate of the transition towards FSVC is lower: that corresponds to maximum time spent in FS due to improper implementation of VC or faulty train-to-train communication channel. On the opposite, with a low rate of faulty conditions in FSVC, we would be closer to the farther corner in the graph (i.e., highest point), where the rate of the transition towards FSVC is very high while the rate of the transition towards FS is much lower. In such a condition, where the trains stay in FSVC most of the time, the graph shows a value close to 100 trains per hour, that is one train each 36 seconds as per our calculations. Any other combinations of mode transition frequencies are possible: for instance, if FSVC is kept very reliably once reached a stationary condition, but the coupling procedure is very slow, then the situation would be the one of the extreme left corner of the graph: around 60 trains per hour that is 1 train per minute, still 3 times better than FS. A similar result (see extreme right corner of the graph) holds if we have an efficient yet unstable transition to FSVC, with trains easily getting from FS to FSVC but also leaving FSVC often, e.g. due to communication faults.

C. The Need for Train-to-Train Communication

If there were no limitations on the performance and reliability of communication channel between train and track-side, then ERTMS Level 3 could support Virtual Coupling to a certain extent by simply setting the *Veoa* variable equal to the speed of the preceding train, as aforementioned. However, as trains get closer (see Fig. 1 (c)), the infrastructure would need to send MA and any emergency messages at ultra-high speeds in order to ensure safe latencies due to extremely short headways. Consequently, engineers should reduce the $T\_NVCONTACT$ vitality timer in proportion to the headway reduction. Today, that timer is set to few seconds to get a good trade-off between safety and performance. In absence of Train-to-Train communication, the timer should be set to fractions of second, scaling down one or two orders of magnitude. That is clearly not compatible with current communication technology used in ERTMS.

Hence, in the rest of this paper we assume that Train-to-Train communication is provided by means of Wi-Fi connection or next-generation networks (e.g., 5G).

Together with train mass and braking capability, actual Virtual Coupling headways will be dependent on train positioning system precision (e.g. odometer error or satellite positioning resolution in future generation ERTMS [15]), which has an influence on the entity of safe margins (i.e. Minimum/Maximum safe Rear/Front End), and on the Train-to-Train connection performance (including bandwidth and stability) together with the availability of appropriate sensors/radars.

IV. Coupling Strategy

A. Communication Topology and Preliminaries

As justified in the previous Section, we assume that trains are equipped with Train-to-Train communication interfaces to share information on their current state (position, velocity, and acceleration). We also assume that the RBC acts as *virtual leader* by dispatching the reference behavior to the other trains under its supervision.

The communication network established among N trains can be modeled by a direct graph $\mathcal{G}_N = (\mathcal{V}_N, \mathcal{E}_N, \mathcal{A}_N)$, where $\mathcal{V}_N = \{1, \ldots, N\}$ is the set of nodes (trains), and $\mathcal{E}_N \subseteq \mathcal{V}_N \times \mathcal{V}_N$ the set of edge (communication links among trains). The topology of the graph is associated to the adjacency matrix $\mathcal{A}_N = [a_{ij}]_{N \times N}$ encoding train communication relationship,

where $a_{ij} = 1$ if $(i, j) \in \mathcal{E}_N$, and $a_{ij} = 0$ otherwise. Note that, $a_{ii} = 0$ since the self-loops (i, i) are not allowed. Moreover, defining the degree matrix as $\Delta = \text{diag}\{\Delta_1, \ldots, \Delta_N\}$, with $\Delta_i = \sum_{j \in \mathcal{V}_N} a_{ij}$, the Laplacian matrix of $\mathcal{G}_N$ is defined a $L_N = \Delta - \mathcal{A}_N$. Furthermore, a *path* of length η in a graph is an ordered sequence of $\eta + 1$ vertices such that any pair of consecutive vertices in the sequence is an edge of the graph. If there exists a path from node i to node j, we say that j is reachable from i.

We consider N trains plus an additional agent representing the RBC labeled with the index zero, i.e. node 0. Then, the resulting network topology is described by a directed graph $\mathcal{G}_{N+1}$. Finally, we assume that node 0 is globally reachable, i.e. always there is a path in $\mathcal{G}_{N+1}$ from every node i in $\mathcal{G}_{N+1}$ to node 0.

B. Control Design

The control design starts with a simplified model of the system. Considering a group of N trains ($i = 1, \ldots, N$) participating to the coupling, we denote the kinematics parameters of the i-th train moving along the track as position r_i [m], velocity v_i [m/s], acceleration a_i [m/s^2] and jerk j_{ei} [m/s^3] measured w.r.t. a railway reference frame. The dynamics can be expressed in the state space as the following third order model [16]:

$$\begin{cases} \dot{r}_i(t) = v_i(t), \\ \dot{v}_i(t) = a_i(t), \\ \dot{a}_i(t) = j_{ei}(t) = -\dfrac{1}{T_i} a_i(t) + \dfrac{1}{T_i} u_i(t). \end{cases} \tag{1}$$

where $T_i > 0$ [s] is the time constant of the drive train depending on the train specific features, while u_i is the desired acceleration to be set to the i-th train to be coupled within a platoon. Since we are dealing with automated longitudinal control, model (1) considers only the actuation lag (i.e., the actual acceleration of the train is assumed to track the desired acceleration with a time constant T_i).

According to the Virtual Coupling paradigm, the reference behavior $\dot{r}_0(t) = v_0$, $\dot{v}_0(t) = a_0 = 0$ (being r_0 [m], v_0 [m/s], and a_0 [m/s^2], reference position, velocity, acceleration) is transmitted to the trains by the RBC. Hence, the Virtual Coupling goal can be expressed as:

$$r_i(t) \to r_0(t) + d_{i0}; \quad v_i(t) \to v_0; \quad a_i(t) \to a_0; \tag{2}$$

where $d_{i0} = h_{i0} v_0 + d_{i0}^{st}$ is the desired distance of the train i from the virtual leader to be set according to the spacing policy, being h_{i0} the time headway (i.e., the time necessary for the train i-th to travel the distance from the leader) and d_{i0}^{st} is the desired distance between vehicles i and the leader 0 at standstill [17]. Note that, with no loss of generality, the spacing policy can be referred to the leading reference since train separation can be expressed as the spacing w.r.t. the reference position $r_0(t)$ [18] provided by the infrastructure.

To achieve the Virtual Coupling goal in (2), we propose the following decentralized control strategy composed of two terms: a local action depending on the state variables of the vehicle (measured on-board) and an action depending on the information received from neighbors and infrastructure. The control protocol embeds the error w.r.t. the reference behavior that trains are forced to reach and keep during the coupling, as well as the time-varying communication delays, as:

$$\begin{aligned} u_i = & -\frac{1}{\Delta_i} \sum_{j=0}^{N} k_{ij} a_{ij} [r_i(t) - r_j(t - \tau_{ij}(t)) - h_{ij} v_0 - d_{i0}^{st}] \\ & - b_i \rho_{i0} [v_i(t) - v_0] - \gamma_i \rho_{i0} a_i(t) \\ & + \frac{1}{\Delta_i} \sum_{j=0}^{N} k_{ij} a_{ij} \tau_{ij}(t) v_0 \end{aligned} \tag{3}$$

where k_{ij}, b_i and γ_i are the control parameters that act as stiffness and damping coefficients to be tuned for regulating the mutual behavior among neighbor trains. Since the strategy is designed to mitigate communication impairments, $\tau_{ij}(t)$ and $\tau_{i0}(t)$ are the time-varying delays affecting the communication with the i-th vehicle when information is transmitted from the vehicle j and the leader, respectively. In general $\tau_{ij}(t) \neq \tau_{ji}(t)$); h_{ij} is the constant time headway (i.e., the time necessary for vehicle i-th to travel the distance separating it from its predecessor); d_{ij}^{st} is the distance between vehicles i and j at standstill. Notoriously [19], delays are assumed to be bounded and detectable. Specifically, we suppose that each train transmits information with a timestamp (i.e., the time instant when the information is sent) so that the communication delay over a link can be estimated by each train when information is received [20]–[22]. Before testing the approach in realistic scenarios (Section V) we need a proof of stability for the coupling protocol.

C. Closed-Loop Stability Analysis

In this section the exponential asymptotic stability of the consensus equilibrium exhibited by trains coupled by the control action (IV) is proven. Note that the use of an exponential criterion not only allows to prove the stability of - or around - the equilibrium solution, but also allows demonstrating the ability in reaching the required virtual coupling regime with an exponentially bounded dynamic behavior. Indeed, while the asymptotic stability of the equilibrium is significant when the coupled trains are moving in steady-state conditions, the exponential stability for delayed systems provides a key ingredient for addressing transient maneuvers in presence of communication delays. That is especially important in the crucial task of coupling engagement (see e.g. [23], [24] for analogous automotive applications).

We define the errors w.r.t. the desired equilibrium (2) as:

$$\begin{aligned} \bar{r}_i &= r_i(t) - r_0(t) - h_{i0} v_0 - d_{i0}^{st}, \\ \bar{v}_i &= v_i(t) - v_0, \\ \bar{a}_i &= a_i(t). \end{aligned} \tag{4}$$

By re-writing the coupling control action u_i in terms of the state errors $\bar{r}_i$, $\bar{v}_i$ and $\bar{a}_i$ and by expressing headway constants h_{ij} and standstill distances d_{ij}^{st} w.r.t. the leading vehicle, namely $h_{ij} = h_{i0} - h_{j0}$ and $d_{ij}^{st} = d_{i0}^{st} - d_{j0}^{st}$, after some algebraic manipulation, the closed-loop dynamics for the generic i-th train within the formation can be rewritten as:

$$\begin{aligned} \dot{\bar{r}}_i(t) &= \bar{v}_i(t), \\ \dot{\bar{v}}_i(t) &= \bar{a}_i(t), \end{aligned}$$

$$\dot{\bar{a}}_i(t) = -\frac{1}{T_i}[\frac{1}{\Delta_i}\sum\nolimits_{j=1}^{N} k_{ij}\alpha_{ij}(\bar{r}_i(t) - \bar{r}_j(t-\tau_{ij}(t))) + b_i\rho_{i0}\bar{v}_i(t) + (1+\gamma_i\rho_{i0})\bar{a}_i(t) + \frac{1}{\Delta_i}k_{i0}\alpha_{i0}\bar{r}_i(t)]. \tag{5}$$

In order to describe train network dynamics in the presence of time-varying delays associated to the communication links in a more compact form, we define the position, speed and acceleration error vectors as $\bar{r} = [\bar{r}_1, \ldots, \bar{r}_N]^\top$, $\bar{v} = [\bar{v}_1, \ldots, \bar{v}_N]^\top$, and $\bar{a} = [\bar{a}_1, \ldots, \bar{a}_N]^\top$; the error state vector as $\bar{x}(t) = [\bar{r}^\top \bar{v}^\top \bar{a}^\top]^\top$ and we furthermore define $\tau_p(t)$, $p = 1, 2, \ldots, m$ (with $m \leq N(N-1)$)) as an element of the sequence $\{\tau_{ij}(t) : i, j = 1, 2, \ldots, N, i \neq j\}$. Note that, m is equal to its maximum, $N(N-1)$, only when the communication topology connecting coupled trains is represented by a directed complete graph and all time-delays are different. The closed-loop train network can be hence represented as the following set of time-delayed differential equations:

$$\dot{\bar{x}}(t) = A_0\bar{x}(t) + \sum_{p=1}^{m} A_p\bar{x}(t-\tau_p(t)), \tag{6}$$

where

$$A_0 = \begin{bmatrix} 0_{N\times N} & I_{N\times N} & 0_{N\times N} \\ 0_{N\times N} & 0_{N\times N} & I_{N\times N} \\ -T\widetilde{K} & -T\widetilde{B} & -\widetilde{T} \end{bmatrix}, \tag{7}$$

$$A_p = \begin{bmatrix} 0_{N\times N} & 0_{N\times N} & 0_{N\times N} \\ 0_{N\times N} & 0_{N\times N} & 0_{N\times N} \\ T\widetilde{K}_p & 0_{N\times N} & 0_{N\times N} \end{bmatrix}, \tag{8}$$

with $0_{N\times N}$ the null matrix of dimension $N \times N$, $T = \text{diag}\{\frac{1}{T_1}, \ldots, \frac{1}{T_N}\}$, $\widetilde{T} = \Omega T$, $\Omega = \text{diag}\{1+\gamma_1\rho_{10}, \ldots, 1+\gamma_N\rho_{N0}\}$, $\widetilde{B} = \text{diag}\{b_1\rho_{10}, \ldots, b_N\rho_{N0}\}$, $\widetilde{K} = \text{diag}\{\widetilde{k}_{11}, \ldots, \widetilde{k}_{NN}\}$ (being $\widetilde{k}_{ii} = \frac{1}{\Delta_i}\sum_{j=0}^{N} k_{ij}\alpha_{ij}$), and $\widetilde{K}_p = [\bar{k}_{pij}] \in \mathcal{R}^{N\times N}$ $(p = 1, \ldots, m)$ as:

$$\bar{k}_{pij}\begin{cases} \dfrac{\alpha_{ij}k_{ij}}{\Delta_i}, & j \neq i, \tau_p(\cdot) = \tau_{ij}(\cdot) \\ 0, & j \neq i, \tau_p(\cdot) \neq \tau_{ij}(\cdot) \\ 0, & j = i. \end{cases} \tag{9}$$

We prove the exponential stability of the closed-loop network in face of communication delays by leveraging on a proper Lyapunov-Krasovskii functional. The approach provides information about the exponential convergence of the error system (i.e. about the creation of the train platoons with a proper timing, or waiting time). The stability conditions for the delayed network is expressed as Linear Matrix Inequality (LMI) criterion that allows the optimization of the convergence rate.

Theorem 1: Consider the delayed closed-loop error system (5). Assume delays $\tau_p(t)$ $(p = 1, \ldots, m)$ to be bounded, i.e. $\tau_p(t) \in [0, \tau_\star]$, $\dot{\tau}_p(t) \in (-\infty, d_p]$ $(\forall t\ \forall p)$ and $d_p \leq 1$. If constants $\delta > 0$, $\psi > 0$, and matrices $P = P^\top > 0$, $Q_p > 0$, $R_p > 0$ $(p = 1, \ldots, m)$ exist so that the following inequality holds

$$[2\delta P + PA_0^\top + PA_0 + \sum_{p=1}^{m} Q_p + \psi\sum_{p=1}^{m} R_p] < 0, \tag{10}$$

with matrix A_0 defined as in (7), then the closed-loop delayed system (5) is exponentially stable with a decay rate δ [25].

Proof 1: Consider the following Lyapunov-Krasovskii functional:

$$V(x_t) = V_1(\bar{x}(t)) + V_2(x_t) + V_3(x_t), \tag{11}$$

where $x_t = \bar{x}(t+\theta), \theta \in [-\tau^\star, 0]$ and

$$V_1(x(t)) = \left(\bar{x}^\top(t)P\bar{x}(t)\right),$$

$$V_2(x_t) = \left(\sum\nolimits_{p=1}^{m}\int_{t-\tau_p(t)}^{t} e^{2\delta(\theta-t)}\bar{x}^\top(\theta)Q_p\bar{x}(\theta)d\theta\right),$$

$$V_3(x_t) = \sum\nolimits_{p=1}^{m}\left(\frac{1}{1-\mu}\int_{t-\tau_p(t)}^{t} e^{2\delta(\theta-t)}\bar{x}^\top(\theta)R_p\bar{x}(\theta)d\theta\right). \tag{12}$$

with $\mu = \max_p(d_p)$ $(p = 1, \ldots, m)$. Following the approach in [4], it can be verified that functional (11) satisfies Lyapunov-Krasovskii stability condition [25].

$$\alpha_1\|\bar{x}(t)\|^2 \leq V(x_t) \leq \alpha_2\|x_t\|^2 \tag{13}$$

with

$$\alpha_1 := \lambda_{min}(P)$$

$$\alpha_2 := \lambda_{max}(P) + \tau^\star\left[\sum\nolimits_{p=1}^{m}\lambda_{max}(Q_p) + \psi\sum\nolimits_{p=1}^{m}\lambda_{max}(R_p)\right] \tag{14}$$

where $\psi = (1-\mu)^{-1}$.

Now, we differentiate each of the terms in (11).

We have:

$$\dot{V}_1(\bar{x}(t)) = \dot{\bar{x}}^\top(t)P\bar{x}(t) + \bar{x}^\top(t)P\dot{\bar{x}}(t) \tag{15}$$

which, after some algebraic manipulation, can be rewritten using (6) as

$$\dot{V}_1(\bar{x}(t)) = \bar{x}^\top(t)[A_0^\top P + PA_0]\bar{x}(t) + 2\bar{x}^\top(t)P\sum_{p=1}^{m} A_p\bar{x}(t-\tau_p(t)). \tag{16}$$

Differentiating $V_2(x_t)$ yields:

$$\dot{V}_2(x_t) = -2\delta V_2(x_t) + \bar{x}^\top(t)\sum\nolimits_{p=1}^{m} Q_p\bar{x}(t) - \sum\nolimits_{p=1}^{m}\Big((1-\dot{\tau}_p(t))\bar{x}^\top(t-\tau_p(t)) \times Q_p\bar{x}(t-\tau_p(t))e^{-2\delta\tau_p(t)}\Big) \tag{17}$$

which, exploiting the bound on the delay functions [26], can be recast as:

$$\dot{V}_2(x_t) \leq -2\delta V_2(x_t) + \bar{x}^\top(t)\sum\nolimits_{p=1}^{m} Q_p\bar{x}(t) - \sum\nolimits_{p=1}^{m}\left(\psi^{-1}\bar{x}^\top(t-\tau_p(t))Q_p\bar{x}(t-\tau_p(t))e^{-2\delta\tau^\star}\right). \tag{18}$$

Analogously, by differentiating $V_3(x_t)$ and by exploiting the bounds on the delay functions, we obtain:

$$\dot{V}_3(x_t) \leq -2\delta V_3(x_t) + \psi \bar{x}^\top(t) \sum_{p=1}^{m} R_p \bar{x}(t) - \sum_{p=1}^{m} \left(\bar{x}^\top(t-\tau_p(t)) R_p \bar{x}(t-\tau_p(t)) e^{-2\delta\tau^\star} \right). \quad (19)$$

Therefore, by using (16), (18), (19), we obtain:

$$\begin{aligned}\dot{V}(x_t) \leq\ & \bar{x}^\top(t)[A_0^\top P + P A_0]\bar{x}(t) + \bar{x}^\top(t) \sum_{p=1}^{m} Q_p \bar{x}(t) \\ & + 2\bar{x}^\top(t) P \sum_{p=1}^{m} A_p \bar{x}(t-\tau_p(t)) - 2\delta V_2(x_t) \\ & - \sum_{p=1}^{m} \left(\psi^{-1} \bar{x}^\top(t-\tau_p(t)) Q_p \bar{x}(t-\tau_p(t)) e^{-2\delta\tau^\star} \right) \\ & - 2\delta V_3(x_t) + \psi \bar{x}^\top(t) \sum_{p=1}^{m} R_p \bar{x}(t) \\ & - \sum_{p=1}^{m} \left(\bar{x}^\top(t-\tau_p(t)) R_p \bar{x}(t-\tau_p(t)) e^{-2\delta\tau^\star} \right).\end{aligned}$$

Summing and subtracting $2\delta V_1(x(t))$ from the right, after some algebraic manipulation, we get:

$$\begin{aligned}&\dot{V}(x_t) + 2\delta V(x_t) \\ &\leq \bar{x}^\top(t)[A_0^\top P + P A_0]\bar{x}(t) \\ &\quad + 2\bar{x}^\top(t) P \sum_{p=1}^{m} A_p \bar{x}(t-\tau_p(t)) + 2\delta \bar{x}^\top(t) P \bar{x}(t) \\ &\quad + \bar{x}^\top(t) \sum_{p=1}^{m} Q_p \bar{x}(t) + \psi \bar{x}^\top(t) \sum_{p=1}^{m} R_p \bar{x}(t) \\ &\quad - \sum_{p=1}^{m} \left(\psi^{-1} \bar{x}^\top(t-\tau_p(t)) Q_p \bar{x}(t-\tau_p(t)) e^{-2\delta\tau^\star} \right) \\ &\quad - \sum_{p=1}^{m} \left(\bar{x}^\top(t-\tau_p(t)) R_p \bar{x}(t-\tau_p(t)) e^{-2\delta\tau^\star} \right).\end{aligned}$$

By defining a new augmented delayed state vector as:

$$\xi(t) = [\bar{x}(t), \bar{x}(t-\tau_1(t)), \ldots, \bar{x}(t-\tau_m(t))]^\top \quad (20)$$

it is possible to recast inequality (20) as:

$$\dot{V}(\xi) + 2\delta V(\xi) \leq \xi^\top(t) \Pi \xi(t), \quad (21)$$

where

$$\Pi = \begin{bmatrix} \Pi_1 & 2PA_1 & \cdots & \cdots & 2PA_m \\ 0_{3N\times 3N} & \Pi_2 & 0_{3N\times 3N} & \cdots & 0_{3N\times 3N} \\ \vdots & 0_{3N\times 3N} & \Pi_3 & \ddots & \vdots \\ \vdots & \vdots & \ddots & \ddots & 0_{3N\times 3N} \\ 0_{3N\times 3N} & \cdots & \ddots & \ddots & \Pi_{m+1} \end{bmatrix} \quad (22)$$

with

$$\begin{aligned}\Pi_1 &= 2\delta P + P A_0^\top + P A_0 + \sum_{p=1}^{m} Q_p + \psi \sum_{p=1}^{m} R_p, \\ \Pi_2 &= -e^{-2\delta\tau^\star}(\psi Q_1 + R_1), \\ &\vdots \\ \Pi_{m+1} &= -e^{-2\delta\tau^\star}(\psi Q_m + R_m),\end{aligned} \quad (23)$$

being $0_{3N\times 3N}$ the null matrix of dimension $3N \times 3N$.

From hypothesis (10), we know that matrix (22) is negative definite. Hence, from (21) we have:

$$\dot{V}(x_t) + 2\delta V(x_t) \leq 0 \implies V(x_t) \leq V(\phi) e^{-2\delta t} \text{ for } t \geq 0. \quad (24)$$

By combining (13) and (24), we obtain [4]:

$$\alpha_1 \|\bar{x}(t; t_0, \phi)\|^2 \leq V(x_t) \leq V(\phi) e^{-2\delta t} \leq \alpha_2 e^{-2\delta t} \|\phi\|_c^2. \quad (25)$$

Hence,

$$\|\bar{x}(t; t_0, \phi)\| \leq \sqrt{\frac{\alpha_2}{\alpha_1}} e^{-\delta t} \|\phi\|_c \quad \text{for } t \geq 0. \quad (26)$$

Therefore, the statement is proven.

Finally, we remark that the LMI (10) that provides the stability region for the control gains is feasible and can be solved numerically, e.g. by a classical interior-point algorithm. Furthermore, for any given control gain set, by leveraging on the LMI-based tuning procedure for exponential stability it is possible to evaluate the achievable decay rate and hence to design the controller to ensure the convergence rate to the closed-loop dynamics.

V. Numerical Analysis

In this section, we apply the proposed Virtual Coupling algorithm to a realistic case study. The goal is to provide a first insight on the possibility of reaching and keeping the reference behavior set by the virtual leader so that all coupled trains can safely move together with a desired velocity and tight spacing. The reference scenario is depicted in Fig. 5. We consider a single RBC (labeled as 0) and three trains with the same mechanical features (numbered from 1 to 3) under its supervision.

Although the on-board control design leverages a simplified linear model of the system to be controlled (namely the one in (1)) to limit control complexity for its real-time implementation, we use a more accurate model of train dynamics. The objective is to test the robustness of the control approach w.r.t. model uncertainties or unknown dynamics (e.g., friction, aerodynamic drag, saturation in the maximum acceleration and traction force, etc.).

The dynamic model describing the motion of the i-th train, assuming train position varying along the route, is given by the following nonlinear system [27]:

$$m_i a_i(t) = F_i - R(v_i(t)) - F_g(r_i(t)) - F_c(r_i(t)), \quad (27)$$

where r_i, v_i and a_i are the train position, velocity and acceleration, respectively; m_i is the train mass; F_i is the bounded tractive or braking force that the traction control have to impose to the i-th train for tracking the desired acceleration profile computed by the coupling protocol $u_i(t)$ in (3); $R(v_i)$ is the resistive force depending on rolling and aero-dynamic resistances, expressed as quadratic function of the velocity according to some empirical parameters known in literature as the Davis parameters, i.e., $R(v_i) = A + B|v_i| + Cv_i^2$; the gradient and curve forces, $F_g(r_i)$ and $F_c(r_i)$, are described respectively as $F_g(r_i) = m_i g \sin(\alpha(r_i))$ and

TABLE I
NUMERICAL ANALYSIS PARAMETERS [28]–[32]

Scenario Parameters	
Maximum trains speed	300 [km/h]
Coupling reference speed	210 [km/h]
Virtual Coupling size	3 trains
Trains max acceleration	0.1 [m/s^2]
Trains max deceleration	-0.6 [m/s^2]
Trains length l_i	190 [m]
Trains mass m_i	380 [tonn]
$F_{i_{\max}}$	208 [N]
Davis parameter A	4.42 10^3 [N]
Davis parameter B	42 [Kg/s]
Davis parameter C	7 [Kg/m]
Control Parameters in Convergence Analysis	
Headway time h_{ij}	0.8 [s] $\forall i, j$
Headway time h_{i0}	0.8 [s] $\forall i$
Distance at standstill d^{st}	50 [m]
Control gains k_{ij}	$k_{10} = 0.01$, $k_{i0} = 0.001$ $(i \neq 0, i \neq 1)$ $k_{i,i-1} = 0.025$, $k_{ij} = 0$ otherwise
Control gains b_i	$b_i = 2$
Control gains γ_i	$\gamma_i = 0.0001$
α_1	0.016
α_2	533.5
Convergence rate	$2\delta = 0.025$

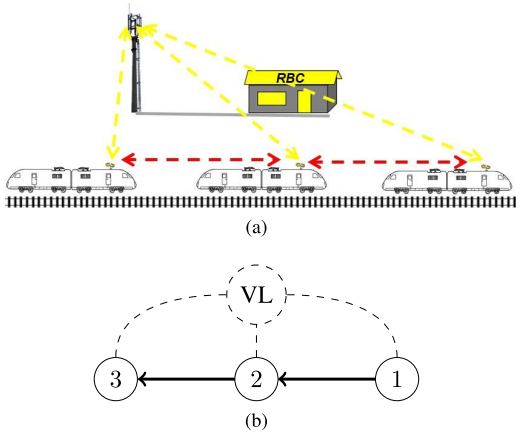

Fig. 5. Virtual Coupling of three trains: (a) Example scenario. (b) Communication topology.

$F_c(r_i) = m_i g k(r_i)/\rho(r_i)$, being g the gravity acceleration, while k, ρ, α are empirical parameters whose values depend on route layout, i.e. curvature radius and track gauge. Parameter α can be positive (i.e. ascent) or negative (i.e., descend). Train and control parameters are reported in Table I. The mechanical characteristics (i.e., maximum speed, acceleration, deceleration, length and mass) are referred to the ETR class of locomotives commonly used on ERTMS lines in Italy (e.g., see [28]–[31] and references therein). Other parameters (i.e., reference coupling-speed, headway and distance at standstill) depend on the specific application and have to be considered as an initial test data since no similar studies have been performed yet for railway applications (see e.g. [32] for automotive applications). Nevertheless, the scenario considers a challenging coupled motion requiring very tight bumper-to-bumper gaps. The numerical simulations have been performed in MATLAB ©, while the Yalmip © Toolbox [33] has been used to tune control gains by solving the LMIs in (10). The multiple time-varying delays along the communication links have been emulated as stochastic variables with a uniform discrete distribution, $\tau_p(t) \in [0, \tau^\star]$ $(p = 1, \ldots m)$ where the maximum value is set above the average end-to-end communication delay typical of IEEE 802.11p vehicular networks [34], i.e., $\tau^\star = 15 \cdot 10^{-2}$ [s].

A. Virtual Coupling Engagement

In order to test and confirm the effectiveness of the theoretical derivation, we consider an example scenario where the coupling command is issued by the RBC when all trains are on a flat track and traveling with similar velocities. We consider that train T_1 has an initial speed of 208 [Km/h], the initial speed of the following train T_2 is 200 [Km/h] and the initial speed of T_3 is 205 [Km/h]. The initial distance between train couples is assumed to be 2000 meters. At time instant 0, the RBC issues the coupling command to the trains. Hence, the two communication links depicted in red in Fig. 5a are established. From that instant of time, the RBC continuously sends the reference speed $v_0 = 210$ [km/h] to the three trains, which in turn share their current position, speed and acceleration via Train-to-Train communication according to a Leader-Predecessor-Follower (LPF) topology as in Fig. 5b. Results in Fig. 6 show that after a transient period the three trains are effectively coupled and equidistant, according to the prescribed spacing policy, and afterward they all run at the steady-state reference speed set by the RBC (see Fig. 6b). As the control gains have been tuned following the LMI- based exponential stability criterion (see parameters in Table I), the trajectories are upper bounded by exponential envelopes, whose decay rate can be estimated according to (26), as shown in Fig. 6a, where the time history of position errors is reported. Results show that according to the theoretical derivation all trains are able to reach and keep the desired formation in 1500 [s] with bounded transient dynamics.

B. Coordinate Emergency Braking Maneuver

Results reported in Fig. 7 represent a more challenging situation when trains are moving as coupled with short gaps and an unpredictable transient maneuver is needed, e.g. emergency braking. In Virtual Coupling such manouvers must be executed in a coordinated fashion so to keep trains coupled while the inter-train distance dynamically changes. Therefore, the spacing policy must be automatically adapted to velocity variations to achieve cooperative coordinate deceleration. The example scenario considers three coupled trains moving on a flat straight track needing to decelerate due to a temporary speed restriction. The RBC sends at time instant $t = 100$ [s] the related information and train start decelerating from their steady-state reference velocity of 210 [Km/h] toward a very low speed of 40 [Km/h]. Results show that the emergency maneuver is safely and automatically executed and all trains correctly follow the trapezoidal breaking profile set by the RBC (see Fig.7a) preserving the bumper-to-bumper spacing as confirmed by time histories of distances and relative speed error in Fig. 7b and Fig. 7c. It is worth noting that during braking inter-train distance dynamically changes according to

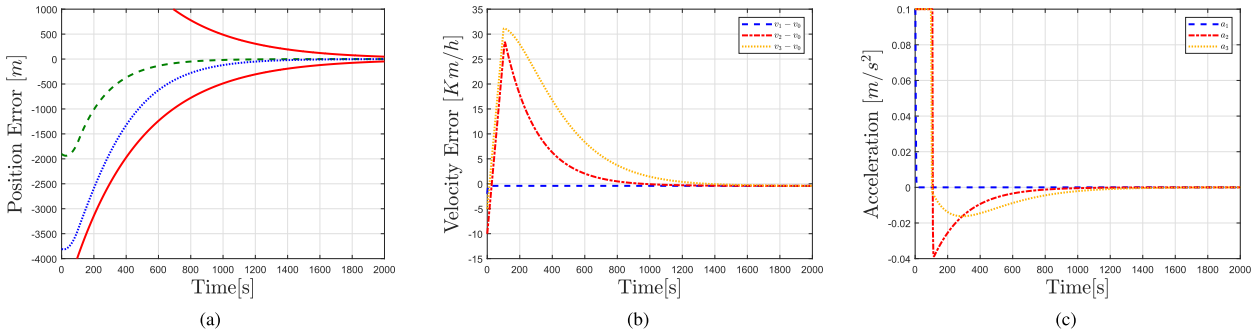

Fig. 6. Couplings creation and maintenance. (a) Time history of the position errors (green dashed line:$r_2(t) - r_1(t) - h_{21}v_0 - d^{st}$; blue dotted line: $r_3(t) - r_1(t) - h_{31}v_0 - d^{st}$), exponential envelops are shown in red). (b) Time history of the speed error with respect to the reference. (c) Time history of the train accelerations.

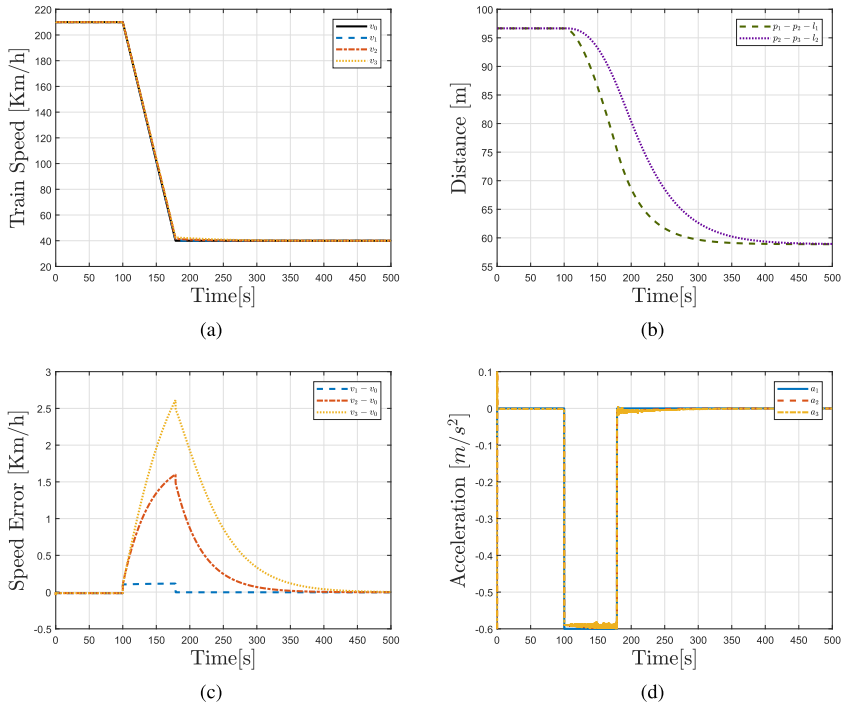

Fig. 7. Emergency Braking. (a) Time history of speed profile. (b) Time history of the bumper-to-bumper distance between the trains. (c) Time history of the speed error. (d) Time history of the train accelerations.

the spacing policy that safely shapes the gaps as the velocity changes (Fig. 7b).

C. Sensitivity to Perturbed Coupling Conditions

In order to investigate the robustness of the control algorithm w.r.t. uncertainties in initial train conditions, different train velocities have also been considered. To that aim, we refer to the coupling engagement maneuver with initial speeds of trains T_1 and T_3 still quite similar, i.e. 208 [Km/h] for T_1 and 205 [Km/h] for T_3, but with train T_2 being much slower, with initial speed of 150 [Km/h]. All trains are initially running at a bumper-to-bumper distance of 2000 [m]. At time 0, the RBC sends the coupling command with a reference velocity of $v_0 = 210$ [Km/h], with trains and the infrastructure communicating via the LPF topology. Results in Figs. 8a and 8b confirm the robustness of the control algorithm since even in perturbed coupling conditions all trains safely reach the coupling goals, with an appropriate settling time below 2000 [s] according to the control tuning for the exponential convergence. Results also show that, as expected, trains automatically implement diverse transient acceleration profiles (e.g. middle train T_2 strongly accelerates due to its low initial velocity) in order to reach the prescribed coupling distances and the required velocity regime.

D. Evaluation of Virtual Coupling in a Real Scenario

In this section we show how to evaluate the Virtual Coupling performance in realistic operating conditions by means of a case study addressing the dynamic response of trains traveling on the Italian ERTMS track connecting Milano to Bologna. The model considers detailed information accounting for the traction effort, dynamic constraints (maximum acceleration

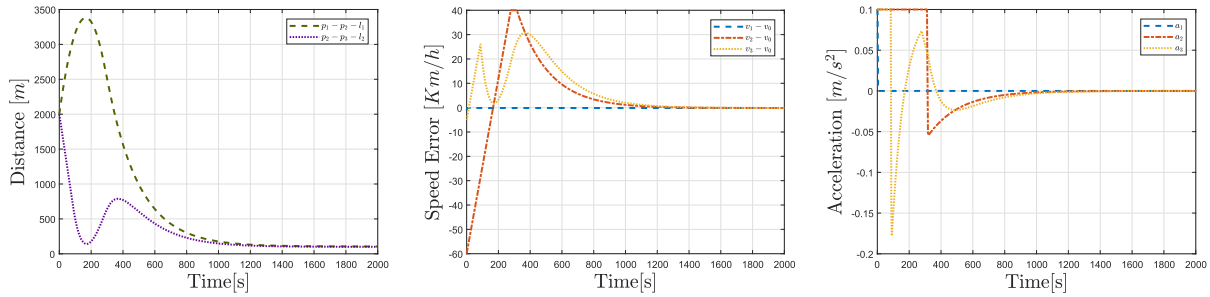

(a) (b) (c)

Fig. 8. Spread in the initial conditions. (a) Time history of the bumper-to-bumper distance between the trains. (b) Time history of the speed error. (c) Time history of the train accelerations.

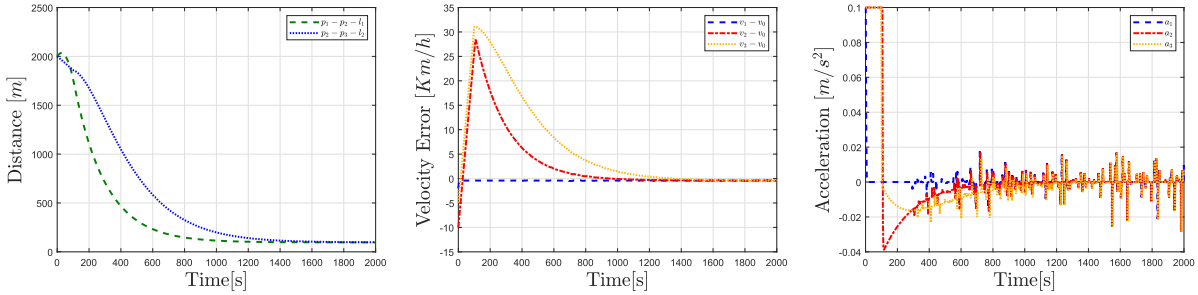

(a) (b) (c)

Fig. 9. Virtual coupling while traveling from Milano to Bologna (Italy). (a) Time history of the bumper-to-bumper distance between the trains. (b) Time history of the speed error. (c) Time history of the train accelerations.

and deceleration), train resistances, and also includes the nonlinear effects due to gradient and curve forces along the route. The goal is to evaluate the ability in reaching and keeping the coupled behavior with three trains in face of nonlinear time-varying disturbances due to the environmental conditions.

Since the autonomous departure and arrival are not to executed in Virtual Coupling, in the scenario we assume that the trains are already traveling when the RBC sends the coupling command and train T_1 is located at a distance of 6 [km] from the start, while trains T_2 and T_3 are at a distance of 4 [km] and 2 [km], respectively, with initial velocities $v_1 = 208$ [km/h], $v_2 = 200$ [km/h] and $v_3 = 205$ [km/h]. Results in Fig. 9 illustrate the coupling engagement maneouver from the initial instant (time 0) when the RBC issues the coupling command. Results confirm that the required dynamic behavior is correctly set to the trains (see Figs. 9a and 9b). As shown in Fig. 9c, the traction force varies according to the control input u_i to counteract the presence of gradient and curve forces as well as of forces depending on rolling and aerodynamic resistances. Acceleration dynamics of all trains are always within admissible bounds despite the changes in track elevation, with a variation that is always below the threshold required for guaranteeing ride comfort and for preventing motion sickness [35].

Regarding implementation related aspects, the target architecture for railways is expected to be similar to the one used in collaborative driving systems in the automotive field. In order to tackle implementation issues coming from time-critical driving applications, connected autonomous vehicles leverage on a stratified architecture including the following layers: vehicle control layer or guidance layer, sensing the environment and controlling the vehicle (traction, brake, etc.) [36]; vehicle management layer, coordinating the vehicles while they are performing maneuvers (such as platooning) based on inter-vehicle communication; traffic control layer, addressing advisory instructions to optimize the traffic flow for each segment (see e.g. [14], [37]–[39]).

VI. Conclusion

We have shown in this paper how railway Virtual Coupling can be implemented by extending the standard set of ERTMS Operating Modes through a proof-of-concept and example numerical analysis. In Full Supervision, when the operational conditions allow Virtual Coupling, the RBC issues to the trains the coupling command acting as a Virtual Leader. Virtual Coupling enables extremely short headways and hence higher track capacity. As demonstrated by the results reported in this paper, appropriate mathematical models and control algorithms borrowed from the automotive field can be employed to prove the effectiveness of cooperative control strategies in reference coupling scenarios and even in degraded scenarios like emergency braking (e.g. line sections out of service). Regardless of the specific results, the numerical analysis and simulation tools provided in this paper allow engineers to evaluate the feasibility and performance of Virtual Coupling in diverse scenarios and operating conditions. Although this paper provides a preliminary analysis of railway Virtual Coupling, the challenges posed by the safe coordination of coupled train convoys open up several future directions as a precondition for real implementation. To that aim, further research efforts are needed to assess the implications of Virtual Coupling in

ERTMS operational scenarios. In particular, the safety-related impact must be investigated further considering new potential hazards. Performance evaluation must also be extended to evaluate the capacity increase in common traffic scenarios, including mixed traffic. Therefore, we plan to study additional scenarios accounting for topology variations, complex maneuvers, as well as to address solutions for fast and reliable Train-to-Train communication.

REFERENCES

[1] *ERTMS/ETCS System Requirements Specification*, UNISIG Standard. SUBSET-026, 2002.

[2] Shift2Rail Joint Undertaking. (2015). *Multi-Annual Action Plan*. [Online]. Available: https://www.shift2rail.org/wp-content/uploads/2013/07/MAAP-final_final.pdf

[3] N. Furness, H. van Houten, L. Arenas, and M. Bartholomeus, "ERTMS Level 3: The game-changer," *IRSE News*, vol. 232, pp. 2–9, Apr. 2017.

[4] L. Hien, Q. P. Ha, and V. N. Phat, "Stability and stabilization of switched linear dynamic systems with time delay and uncertainties," *Appl. Math. Comput.*, vol. 210, no. 1, pp. 223–231, Apr. 2009.

[5] I. Mitchell *et al.*, "ERTMS level 4, train convoys or virtual coupling," *Int. Tech. Commitee*, vol. 219, pp. 1–3, Feb. 2016.

[6] J. Goikoetxea, "Roadmap towards the wireless virtual coupling of trains," in *Proc. Int. Workshop Commun. Technol. Vehicles*, May 2016, pp. 3–9.

[7] B. Ai *et al.*, "Challenges toward wireless communications for high-speed railway," *IEEE Trans. Intell. Transp. Syst.*, vol. 15, no. 5, pp. 2143–2158, Oct. 2014.

[8] J. Moreno, J. M. Riera, L. de Haro, and C. Rodriguez, "A survey on future railway radio communications services: Challenges and opportunities," *IEEE Commun. Mag.*, vol. 53, no. 10, pp. 62–68, Oct. 2015.

[9] P. Unterhuber, A. Lehner, and F. de Ponte Müller, "Measurement and analysis of ITS-G5 in railway environments," in *Proc. Int. Workshop Commun. Technol. Vehicles*, May 2016, pp. 62–73.

[10] P. Fraga-Lamas, T. M. Fernández-Caramés, and L. Castedo, "Towards the Internet of smart trains: A review on industrial IoT-connected railways," *Sensors*, vol. 17, no. 6, p. 1457, Jun. 2017.

[11] D. Jia, K. Lu, J. Wang, X. Zhang, and X. Shen, "A survey on platoon-based vehicular cyber-physical systems," *IEEE Commun. Surveys Tuts.*, vol. 18, no. 1, pp. 263–284, 1st Quart., 2016.

[12] S. Santini, A. Salvi, A. S. Valente, A. Pescapé, M. Segata, and R. L. Cigno, "A consensus-based approach for platooning with inter-vehicular communications and its validation in realistic scenarios," *IEEE Trans. Veh. Technol.*, vol. 66, no. 3, pp. 1985–1999, Mar. 2017.

[13] M. di Bernardo, A. Salvi, and S. Santini, "Distributed consensus strategy for platooning of vehicles in the presence of time-varying heterogeneous communication delays," *IEEE Trans. Intell. Transp. Syst.*, vol. 16, no. 1, pp. 102–112, Feb. 2015.

[14] R. Hult *et al.*, "Design and experimental validation of a cooperative driving control architecture for the grand cooperative driving challenge 2016," *IEEE Trans. Intell. Transp. Syst.*, vol. 19, no. 4, pp. 1290–1301, Apr. 2018.

[15] F. Rispoli. (2013). *GNSS for Train Control Systems*. [Online]. Available: https://www.gsa.europa.eu/sites/default/files/APPAP_Workshop_Ansaldo_0.pdf

[16] R. Rajamani, *Vehicle Dynamics and Control*. Boston, MA, USA: Springer, 2011.

[17] G. J. L. Naus, R. P. A. Vugts, J. Ploeg, M. J. G. van de Molengraft, and M. Steinbuch, "String-stable CACC design and experimental validation: A frequency-domain approach," *IEEE Trans. Veh. Technol.*, vol. 59, no. 9, pp. 4268–4279, Nov. 2010.

[18] M. di Bernardo, P. Falcone, A. Salvi, and S. Santini, "Design, analysis, and experimental validation of a distributed protocol for platooning in the presence of time-varying heterogeneous delays," *IEEE Trans. Control Syst. Technol.*, vol. 24, no. 2, pp. 413–427, Mar. 2016.

[19] G. Chen and F. L. Lewis, "Leader-following control for multiple inertial agents," *Int. J. Robust Nonlinear Control*, vol. 21, no. 8, pp. 925–942, 2011.

[20] F. Librino, M. E. Renda, and P. Santi, "Multihop beaconing forwarding strategies in congested IEEE 802.11p vehicular networks," *IEEE Trans. Veh. Technol.*, vol. 65, no. 9, pp. 7515–7528, Sep. 2016.

[21] J. Mittag, F. Thomas, J. Härri, and H. Hartenstein, "A comparison of single-and multi-hop beaconing in VANETs," in *Proc. 6th ACM Int. Workshop VehiculAr InterNETworking*, Sep. 2009, pp. 69–78.

[22] H. Venkataraman, A. D'Ussel, T. Corre, C. H. Muntean, and G. M. Muntean, "Performance analysis of real-time multimedia transmission in 802.11p based multihop hybrid vehicular networks," in *Proc. 6th Int. Wireless Commun. Mobile Comput. Conf.*, Jun. 2010, pp. 1151–1155.

[23] C. Nowakowski, D. Thompson, S. E. Shladover, A. Kailas, and X.-Y. Lu, "Operational concepts for truck maneuvers with cooperative adaptive cruise control," *Transp. Res. Rec.*, vol. 2559, no. 1, pp. 57–64, 2016.

[24] L. Stranden, "A framework for complex scenarios for vehicle platoons," in *Proc. IEEE 18th Int. Conf. Intell. Transp. Syst.*, Sep. 2015, pp. 2186–2193.

[25] K. Gu, V. L. Kharitonov, and J. Chen, *Stability of Time-Delay Systems*. Boston, MA, USA: Springer, 2003.

[26] E. Fridman and Y. Orlov, "Exponential stability of linear distributed parameter systems with time-varying delays," *Automatica*, vol. 45, no. 1, pp. 194–201, Jan. 2009.

[27] A. Albrecht, P. Howlett, P. Pudney, X. Vu, and P. Zhou, "The key principles of optimal train control—Part 1: Formulation of the model, strategies of optimal type, evolutionary lines, location of optimal switching points," *Transp. Res. Part B, Methodol.*, vol. 94, pp. 482–508, Dec. 2016.

[28] *ETR460-463 Class of Locomotives. Technical Sheet*. Accessed: Apr. 16, 2019. [Online]. Available: http://www.leferrovie.it/leferrovie/wiki/doku.php?id=schede_tecniche:start

[29] International Union of Railway. *High-Speed Locomotives. Technical Sheet*. Accessed: Apr. 16, 2019. [Online]. Available: https://uic.org/IMG/pdf/high_speed_brochure.pdf

[30] Italian State Railways. *High-Speed Locomotives. Technical sheet*. Accessed: Apr. 16, 2019. [Online]. Available: https://www.fsitaliane.it/content/dam/fsitaliane/Documents/media-ed-eventi/comunicati-stampa-e-news/anno-2017/ottobre/2017_10_10_scheda_tecnica_pop.pdf

[31] A. Steimel, *Electric Traction-Motive Power and Energy Supply: Basics and Practical Experience*. Munich, Germany: Oldenbourg Industrieverlag, 2008.

[32] S. E. Li, Y. Zheng, K. Li, L.-Y. Wang, and H. Zhang, "Platoon control of connected vehicles from a networked control perspective: Literature review, component modeling, and controller synthesis," *IEEE Trans. Veh. Technol.*, to be published.

[33] J. Lofberg, "YALMIP: A toolbox for modeling and optimization in MATLAB," in *Proc. IEEE Int. Conf. Robot. Automat.*, Sep. 2004, pp. 284–289.

[34] W. Alasmary and W. Zhuang, "Mobility impact in IEEE 802.11p infrastructureless vehicular networks," *Ad Hoc Netw.*, vol. 10, no. 2, pp. 222–230, 2012.

[35] J. Förstberg, "Ride comfort and motion sickness in tilting trains. Human responses to motion environments in train and simulator experiments," Ph.D. dissertation, Royal Inst. Technol., Stockholm, Sweden, 2000.

[36] Y.-D. Song, Q. Song, and W.-C. Cai, "Fault-tolerant adaptive control of high-speed trains under traction/braking failures: A virtual parameter-based approach," *IEEE Trans. Intell. Transp. Syst.*, vol. 15, no. 2, pp. 737–748, Apr. 2014.

[37] S. Tsugawa, S. Kato, T. Matsui, H. Naganawa, and H. Fujii, "An architecture for cooperative driving of automated vehicles," in *Proc. IEEE Intell. Transp. Syst.*, Oct. 2000, pp. 422–427.

[38] S. Hallé and B. Chaib-Draa, "Collaborative driving system using teamwork for platoon formations," in *Proc. Appl. Agent Technol. Traffic Transp.*, Mar. 2005, pp. 133–151.

[39] A. Morales and H. Nijmeijer, "Merging strategy for vehicles by applying cooperative tracking control," *IEEE Trans. Intell. Transp. Syst.*, vol. 17, no. 12, pp. 3423–3433, Dec. 2016.

Carlo Di Meo received the M.Sc. degree in control systems engineering from the University of Naples Federico II, Naples, Italy, in 2017. He is currently a Junior Research Fellow with the Department of Electrical Engineering and Information Technology, University of Naples Federico II. His research interests include intelligent transportation systems and communication-based train control.

Marco Di Vaio received the M.Sc. degree in control systems engineering from the University of Naples Federico II, Naples, Italy, in 2017. He was a Visiting Student with the Chalmers University of Technology, Göteborg, Sweden, in 2016. He is currently a Research Fellow with the Department of Electrical Engineering and Information Technology, University of Naples Federico II. His research interest includes the distributed control applied to autonomous driving and cooperative systems.

Francesco Flammini received the M.D. and Ph.D. degrees in computer engineering from the University of Naples Federico II, in 2003 and 2006, respectively. He is currently a Senior Lecturer with Linnaeus University, Sweden. He has a long industry experience working on international research projects addressing ERTMS/ETCS and critical infrastructures, including the EU funded projects, named PilotSHIELD and NewSHIELD, specializing on the dependability of embedded systems in railway applications.

Roberto Nardone received the M.D. and Ph.D. degrees in computer engineering from the University of Naples Federico II, Naples, Italy, in 2009 and 2013, respectively. He is currently a Post-doctoral Fellow with the University of Naples Federico II. His research interests include quantitative evaluation of non-functional properties, with a particular focus on dependability and performability assessment and threat propagation analysis, by means of model-based and model-driven techniques. He is involved in research projects with academic and industrial partners.

Stefania Santini received the M.Sc. degree in electronic engineering and the Ph.D. degree in automatic control from the University of Naples Federico II, Naples, Italy, in 1996 and 1999, respectively. She is currently an Associate Professor in automatic control with the University of Napoli Federico II. Her research interests include analysis and control of nonlinear, networked, and delayed systems with applications to computational biology, energy, automotive engineering, and transportation technologies. She is involved in many projects with industry, including SMEs operating in the automotive field.

Valeria Vittorini received the M.D. degree in mathematics and the Ph.D. degree in computer engineering from the University of Naples Federico II, in 1991 and 1995, respectively. She has been an Associate Professor with the University of Naples Federico II, since 2005. She teaches computer programming, formal modeling, and workflow and process automation. Her current research interests include dependability and performance evaluation of computer systems, validation and verification of critical systems, and critical infrastructures protection with a special focus on railway transportation systems.